IV INTERNATIONAL SCIENTIFIC FORUM
"NUCLEAR SCIENCE AND TECHNOLOGIES"
dedicated to the 65th anniversary of the RSE INP
14th International conference
"Nuclear and Radiation Physics"
3rd International conference
"Nuclear and Radiation Technologies in Medicine, Industry and Agriculture"
September 26-30, 2022
Almaty, Republic of Kazakhstan

EVALUATION OF THE EFFECT OF SELF-SHIELDING ON THE ABSORBED DOSE IN NCT

Kulabdullaev G.A, Abdullaeva G.A, Kim A.A, YuldashevDj.O, Khamidov Kh.Z, Zokirov Ch.U.

Institute of Nuclear Physics of the Academy of Sciences of Uzbekistan, Tashkent

Annotation. The successful use of neutron capture therapy (NCT) depends on an accurate assessment of the absorbed dose in the tumor. And the absorbed dose depends on the exact determination of the neutron spectra at the target location. As is known, when a flux of epithermal neutrons passes through a substance, the flux decreases. When planning GdNCT, to accurately determine the absorbed dose it is necessary to consider the effect of attenuation (self-shielding) of the beam in the element itself (Gd), which is used to enhance the absorbed dose in the tumor. Calculations were made to determine the effect of Gd self-shielding with Magnevist in the human brain d=7.5 cm and tumor d=4.5 cm. Three spheres d=1.2 cm located inside the tumor were selected for calculations. Calculations showed that, in peripheral tumors, the self-shielding effect begins to affect from a concentration of 1000 ppm, in deeper tumors, the self-shielding effect begins to affect at low concentrations. At high concentrations of Gd, the power of photon doses increases, which can be used for therapy. For a more thorough study of this issue, further research is required.

Introduction

Neutron capture therapy (NCT) is a binary radiotherapy method that allows maximum preservation of healthy cells that enter the irradiation zone. NRT combines a specific preparation labeled with ^{10}B or ^{157}Gd and a low-energy neutron beam sufficient to capture neutrons in the treated tissues. These two therapeutic components are harmless on their own, while their combination results in a highly localized and lethal radiotoxic response at the cellular level. At

present, these two methods of NCT (BNCT and GdNCT) are being developed at different levels. Estimation of the absorbed dose for treating BNCT using epithermal neutrons in deep tumors is a difficult task. A feature that causes inaccuracies in determining the dose is the dependence of the thermal neutron fluence ϕ_{th} on the size and shape of the irradiated volume, as well as on the direction of the incident beam. Therefore, the therapeutic dose D_B obtained from reactions of 10B with thermal neutrons ($^{10}B(n_{th}, \alpha)\ ^{7}Li$) and the dose of gamma radiation D_γ, mainly obtained from reactions of thermal neutrons with hydrogen ($^{1}H(nth, \gamma)\ ^{2}H$) , also depend on the shape and size of the irradiated volume. The dose due to collisions of fast neutrons (D_{fast}), in contrast to D_B and D_γ, does not strongly depend on the geometry of the irradiated volume, except for the peripheral regions. Due to the short range of α and ^{7}Li charged particles, the therapeutic dose D_B is proportional to ϕ_{th} and can be estimated at each position using the neutron kerma factor. In contrast, due to the large path in the tissue of photons with an energy of 2.2 MeV emitted in reactions of thermal neutrons with hydrogen, D_γ has a spatial distribution different from the distribution of ϕ_{th}, and undergoes greater changes than that of DB, due to a change in shape or size-irradiated volume. The following data were obtained in [1]: (i) the change in the neutron spectrum depending on the depth in water, (ii) the fluence profiles of thermal and epithermal neutrons in phantoms of different shapes or sizes and with different directions of beam incidence, and (iii) D_γ profiles in various phantoms information is obtained as a function of phantom depth and distance from the beam axis. The calculated and experimental results agree. The results obtained using various phantoms showed significant dependence of ϕ_{th} and D_γ on the geometry of the phantom. The results the work provide useful information that allows a preliminary assessment of the degree of inaccuracy that may result from inaccurate geometry settings in treatment planning. In T. Kobayashi et al. [2], the absorbed dose characterization in BNCT is determined by an evaluation procedure that is divided into (i) cell level and (ii) organ level. Uncertain conditions are indicated when assessing the absorbed dose at the cellular level in BNCT. Boron distribution data were measured by PET image analysis using ^{18}F-BPA. The distribution of the absorbed dose at the organ level is estimated using the calculated distribution of the neutron flux. But there are few measurement data during BNCT. This may more clearly explain the relationship between the measured absorbed dose at the organ level and the therapeutic effect of BNCT. A. Zaboronok et al. [3] were the first to develop a method for assessing the absorbed dose in a sample using gold and boron compounds accumulated in glioma cells. Hybrid nanoparticles of gold and boron were also presented and their role was shown both in tumor ablation and in direct measurement of radiation dose. The authors believe that such nanoparticles can be additionally used to visualize the distribution of compound boron in tumor tissues using isotope scanning or single photon emission spectroscopy (SPECT) to obtain data on the absorbed dose of neutrons during BNCT. In the work of H. Koivunoro et al.[4] the extended isoeffective photon dose formalism was applied to calculate normal tissue complication probability (NTCP) for mucosal surfaces in patients with recurrent head and neck carcinoma who were treated with BNCT in a phase I/II clinical trial in Finland from 2003 to 2011. Mucosal membranes are known to be radiosensitive (BEC = 2.5) and the absorbed mucosal dose is often the limiting dose factor. The likelihood of complications was compared with the probabilities derived from conventional OBE doses. The results showed that the isoeffective photon dose model predicted mucosal toxicity after BNCT more reliably than the traditional RBE model or physically absorbed doses. Evaluation of mucosal toxicity in more patients is needed to confirm results.

In the work of S. Gonzalez et al. [5] Comparing BNCT with photon radiation therapy requires a dose calculation model that predicts an adequate "photon equivalent" value. The authors reported that the standard BNCT dose calculation model, which uses fixed RBE/CBE factors, results in unrealistically high RBE-weighted tumor doses. A more acceptable approach has been presented that defines the isoeffective photon dose as a reference dose that provides the same level of cell survival as a given combination of absorbed dose components in BNCT. This formalism, with radiobiological parameters derived from the metastatic human melanoma cell line Mel-J, was applied to re-evaluate dosimetry in the cutaneous melanoma BNCT study in Argentina. The results showed that the standard approach was unsuitable for explaining the observed result.

Isoeffective photon doses obtained using in vitro radiobiological parameters for analyzed patients were 7–46% lower than RBE-weighted tumor doses. These results confirm the authors' previous assertions that RBE-weighted tumor doses often overestimate the actual photon equivalent values. In addition, dose estimates based on in vitro and in vivo data show agreement with differences of less than 5%. Finally, the most probable value of controlled tumors coincides with the observed result only for isoeffective photon doses.

Early studies on BNCT often ignored the self-shielding effects caused by ^{10}B accumulation in tumors. This led to an overestimation of the actual delivered dose to the tumor. In the work of Sung-Joon Ye [6], the self-shielding effect of boron was calculated from the viewpoint of reducing the thermal neutron flux through the brain and dose delivered in tumors. The calculated differences for ^{10}B concentrations of 7,5–30 ppm are 2,3%–8.3% at a depth of 2,3 cm ~ the depth of the maximum dose of the brain and 4,6%–17% at a depth of 7,3 cm ~ in the center of the brain. Additional self-shielding effects on the concentration of ^{10}B in a bulk tumor were studied for a spherical tumor 3 cm in diameter located either near the surface at a depth of ~3,3 cm or in the center of the brain at a depth of ~7,3 cm along the midline of the fascicle. For 45 ppm ^{10}B in the tumor and 15 ppm ^{10}B in the brain, the dose delivered to tumors is about 10% lower at 3,3 cm and 20% lower at the center of the brain compared to the dose without boron self-shielding in the calculations. In [7], the method of activation detectors was used to measure neutron spectra. The energy region of epithermal neutrons imposes a resonant structure of activation cross sections, which leads to strong self-shielding effects. The correction factor for neutron self-shielding was calculated using a simple analytical model of a single absorption event. This procedure was applied to individual cross sections from the ENDF/B-VI dot library, and new corrected activation cross sections were introduced into the spectrum-unfolding algorithm. The method was verified experimentally for both isotropic and parallel neutron beams. Two sets of dilute and undiluted cadmium-coated activation foils were irradiated in a neutron field. Comparison of the activation rates of dilute and undiluted foils showed the accuracy of the self-shielding model used.

In [8], the self-shielding effect of Gd was confirmed by calculations using MCNP for modeling and when measuring the dose of gadolinium with Fricke chemical dosimeters. Despite these studies, due to the self-shielding effect of the ^{10}B or ^{nat}Gd elements used, the issue of accurately determining the absorbed dose in NRT remains open. Therefore, the study of the correlation of the clinical response of malignant tumors with the absorbed dose, conducted in the work of H. Koivunoro et al. [9] is very relevant. The correlation of clinical tumor response was studied in 89 patients with inoperable the previously irradiated head and neck cancer. The values of the total equivalent dose of radiation during photon radiotherapy for the tumor were obtained by multiplying the dose component by the value of the relative biological effectiveness (RBE) and for the dose of boron by the biological effectiveness compound (BEC) [10]. The most favorable

middle survival time (MST) obtained using BNCT to date has been 27,1 months. This result was obtained by Matsumura et al. at Tsukuba University Hospital [11–13] using either BPA or BSH alone or in combination. In some cases, BNCT has been combined with photonic support along with temozolomide in patients with either primary or current glioblastoma multiforme (GBM).

Research method

Determining the required concentration of elements (^{10}B or ^{nat}Gd) for NCT is an unresolved problem. Because of this problem, and because of the self-shielding effect of the elements used, the issue of accurately determining the absorbed dose in NCT remains open. To understand the scale of this problem, it is expedient to consider the physical processes that occur when tumors are irradiated with epithermal neutrons.

The law of decreasing neutron flux, if x is the distance, can be represented by the formula:

$$\Phi(x) = \Phi_0 e^{-x/\lambda}$$

where Φ_0 is the flux that falls on the front of the tumor, λ is the mean free path of particles in the substance, which determines the probability of neutron interaction with the substance. Based on this definition of the free path *l* (the dimension of *l* is [cm], the length of the free path has the dimension of length), we can say that it is the reciprocal of the macroscopic cross-section. If the concentration of nuclei has become twice as large, then the mean free path has become twice less.

The same can be said about the microscopic section, which is why it turns out that both of these quantities in the product behave in the same way, inversely proportional to l, therefore the macroscopic section is the reciprocal of the mean free path and vice versa. Given that for a full macroscopic section, one can write:

$$\Sigma_t = \Sigma_f + \Sigma_c + \Sigma_s$$

To obtain a large dose in the tumor, a large concentration of gadolinium is required. Let us determine the average pathway λ_t that the neutron passes before the interaction, considering the medium to be infinite

$$\lambda_t = \frac{\int_0^\infty z \cdot \exp(-\Sigma_{tot} \cdot z) dz}{\int_0^\infty \exp(-\Sigma_{tot} \cdot z) dz} = \frac{1}{\Sigma_{tot}} .$$

If the density of neutrons with velocity V is equal to n, the number of interactions in 1 cm^3 per 1 s (reaction rate) is determined by the relation:

$$R = \frac{n}{\Delta t} = n \cdot \langle V \rangle \cdot \Sigma = \Phi \cdot \Sigma ,$$

where Φ is the neutron flux density, and sigma is the large macroscopic cross-section.

These arguments are correct if the neutron beam consists only of epithermal neutrons. The reactor beams of epithermal neutrons contain fast neutrons and photons. Therefore, to consider the total contribution of these radiations, we performed a calculation using the MCNP-4C program.

Results, discussion and conclusion

As we noted in [14], the radiation used in NCT is a mixed complex radiation with high and low linear energy transfer (LET). This depends on the spatial, spectral, and angular characteristics of the incident neutron radiation, as well as on the geometry and elemental composition of the target. The absorbed dose in GdNCT can be divided into four primary dose components: doses from thermal neutrons, fast neutrons, photons, and natural gadolinium. The primary thermal neutron dose is the result of the thermal neutron capture reaction in 14 N

$$^{14}_{7}N + ^{1}_{0}n \rightarrow ^{14}_{6}C + ^{1}_{1}H + 0{,}66\ МэВ$$

It includes 96% neutron kerma ICRU 46 of brain tissue [15] below 0.5 eV of the thermal neutron cutoff energy.

The fast neutron dose results primarily from the elastic collision of neutrons with hydrogen:

$$^{1}_{1}H + ^{1}_{0}n \rightarrow ^{1}_{1}H + ^{1}_{0}n'$$

It represents 90% of adult brain kerma between 600 eV and 3 MeV.

Other reactions caused by neutrons with energies from 40 eV to 5 MeV, primarily in ^{12}C, ^{16}O and ^{31}P contribute 4%-8% to the brain kerma, but certain resonant energies can contribute more. The components of the photon dose come from two components, the accompanying photons in the neutron beam incident on the target, and the gamma quanta produced by neutron capture reactions. In GdNCT, the main contribution to the absorbed dose comes from the ^{155}Gd and ^{157}Gd isotopes, which have a large neutron capture cross-section with thermal neutron capture cross sections of 60,800 and 255,000 barn, respectively, which are approximately 16 and 66 times greater than the capture cross-section of ^{10}B. Nuclear reaction cross sections for other isotopes are small, which can be neglected in absorbed dose calculations. Therefore, many authors consider that nuclear reactions in these isotopes are the main contributor to the final dose (20% - ^{155}Gd and 80% -^{157} Gd) of natural Gd:

$$^{157}_{64}Gd + ^{1}_{0}n \rightarrow ^{158}_{64}Gd + \gamma + 7{,}94\ МэВ$$

$$^{155}_{64}Gd + ^{1}_{0}n \rightarrow ^{156}_{64}Gd + \gamma + 8{,}54\ МэВ$$

In this reaction, in addition to high-energy γ-rays, internal conversion electrons, X-rays and Auger electrons are produced. According to [16], in this case, gamma rays are reproduced with energies from 0,079 MeV to 7,88 MeV, the energy of internal conversion electrons is 45–66 keV, Auger electrons are 5–9 keV, X-rays are 10,7–38,4 keV in the neutron capture reaction in ^{157}Gd. In the ^{155}Gd at (n,γ) - reactions, ^{156}Gd levels are excited 60,01; 86,546; 107,584; 117,998; 121,1 and 146,21 keV, which have sufficient conversion factors to cause other emissions; ^{157}Gd at (n,γ) - reactions are exciting by levels of ^{158}Gd 54,536; 63,916; 115,717 and 180,224 keV that also have sufficient conversion factors to cause other emissions, which then falls apart. At present, there are no accurate estimates of these emissions. The available data essentially differ from each [17–23]. An Accurate measurement of the absorbed dose in biological tissues is a difficult experimental problem.

In MCNP calculations, all physical processes are considered, which include the creation, absorption and scattering of neutrons, photons and electrons when interacting with the atomic nuclei of the medium because of nuclear reactions. The input data are the location of the sources

and their emission spectra, as well as the geometry and composition of the materials of the medium. Reaction probabilities are calculated using libraries of effective reaction cross sections, which are also included in the MCNP software package. In MCNP programs, these calculations can be performed using tally 4 and tally 6, which are evaluated to the following value [24]:

$$F_4 = \iiint_{VtE} \Phi(\vec{r}, E, t) dE dt \frac{dV}{V}$$

Using the KERMA approximation, the dose can be represented using the following equation [24]:

$$F_{6,7} = \frac{\rho_a}{\rho_g} \iiint_{VtE} H(E) \Phi(\vec{r}, E, t) dE\ dt\ \frac{dV}{V}$$

where ρα is the density of atoms (atom/barn · cm), ρg is the density in grams (g/cm3).
H(E) is the heating response (summed over the nuclides in the material).
Using the KERMA approximation, the dose can be represented using the following equation [24]:

$$D\left(\frac{Gy}{source\ particle}\right) = \frac{C}{N} \sum_{j=1}^{N} \sum_{i=1}^{T} \phi \sigma_T(E) H(E),$$

$$\text{where } C = \left(1.602x10^{-10} \frac{Gy}{Mev/g}\right)\left(1x10^{-24} \frac{cm^2}{barn}\right)\left(\frac{N_a \eta}{M}\right).$$

Where: N_a- Avogadro's Number=6,022x10 23 mol-1; η is the number of atoms in a molecule; M is the molar mass of the material in grams; φ - fluence, particle/cm2; σT is the total atomic cross-section at track energy in barns; H = heating number in MeV per collision at track energy; N = number of original particles; T = number of tracks of initial particles;
MCNP calculations were carried out for human brain tumors d=4.5 cm located on the beam of epithermal neutrons of the Institute of Nuclear Physics of the Academy of Sciences of the Republic of Uzbekistan. This geometry was chosen for the convenience of calculations. The calculation geometry is shown in Figures 1–3.

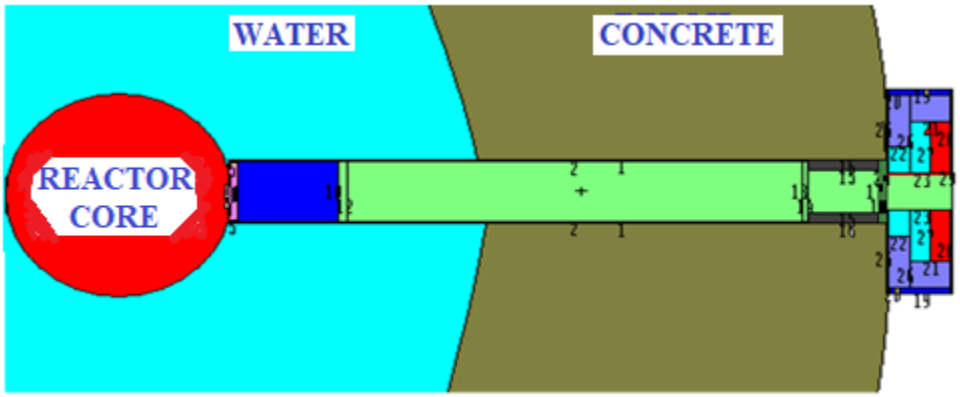

Fig.1 Scheme of the horizontal channel for calculations

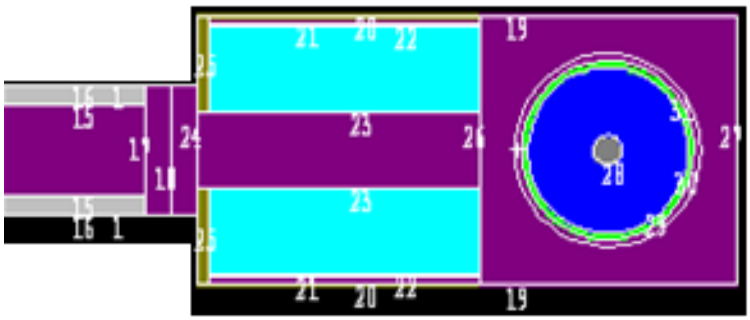

Fig.2 MCNP collimator scheme and human head model for calculations

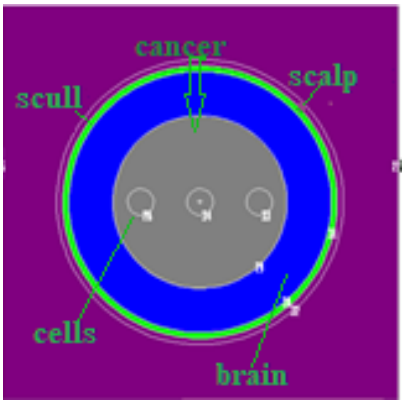

Fig.3. Head model with a tumor in the center of the head and calculation cells

Table 2 shows the results of calculations with the MCNP-4C program.

Table 2. Results of calculations using the MCNP-4C program

The amount of ^{nat}Gd in the tumor	Cell	Dose rate, $\times 10^{-4}$	Relative error MCNP	Dose rate, $\times 10^{-6}$	Relative error MCNP
no ^{nat}Gd	26	1,71884	0,0145	2,66337	0,3146
	27	1,15563	0,0176	1,43764	0,2215
	28	1,37547	0,0147	2,05519	0,1970
	29	4,05908e-2	0,0331	4,26558e-1	0,1688
	30	3,02744e-2	0,0207	2,59741e-1	0,1600
1ppm	26	1,71877	0,04473	2,66320	0,3146
	27	1,15624	0,04472	1,43756	0,2215
	28	1,37682	0,01470	2,05507	0,1970
	29	4,06655e-2	0,0331 0	4,26533e-1	0,1688
	30	3,03065e-2	0,02070	2,59725e-1	0,1600
10ppm	26	1,71813	0,0145	2,64939	0,3165
	27	1,15340	0,0175	1,40186	0,2259
	28	1,37571	0,0147	1,94970	0,2016
	29	4,08264e-2	0,0330	4,24592e-1	0,1701
	30	3,04012e-2	0,0207	2,57987e-1	0,1612
100ppm	26	1,71712	0,0146	4,04305	0,3056
	27	1,15093	0,0173	1,45995	0,2265
	28	1,38242	0,0152	2,25939	0,1865
	29	4,1370e-2	0,0344	5,2773e-1	0,1824
	30	3,05766e-2	0,0209	2,93665e-1	0,1580
1000ppm	26	1,72080	0,0146	4,04437	0,3056
	27	1,15041	0,0173	1,54509	0,2210
	28	1,38390	0,0152	2,30180	0,1845
	29	4,16188e-2	0,0344	5,30882e-1	0,1814
	30	3,06330e-2	0,0209	2,95082e-1	0,1574
10000ppm	26	1,68773	0,0139	3,50670	0,2975
	27	1,15521	0,0167	1,41989	0,2240
	28	1,39369	0,0150	2,96665	0,1521

	29	4,09923e-2	0,0345	7,33780e-1	0,1458
	30	3,05290e-2	0,0210	4,22827e-1	0,1425
50000ppm	26	1,65466	0,0141	6,97570	0,1358
	27	1,20355	0,0154	3,29090	0,1599
	28	1,39700	0,0152	4,65108	0,1666
	29	3,8130e-2	0,0339	1,22931	0,0904
	30	2,9008e-2	0,0190	4,92459e-1	0,0839

Cells 26, 27 and 28 are spheres with a size of d=1.2 cm in the tumor, which are located inside the tumor, starting from the edge (see Fig. 3). Cell 29 is the rest of the tumor that did not enter cells 26, 27, 28 and 30 cell is the brain of a person with a tumor d = 4.5 cm. Table 2 shows that the neutron dose rate in cell 26 first imperceptibly drops to 100 ppm and begins to grow at a Gd concentration of 1000 ppm. At high concentrations, the neutron dose rate begins to fall. The dose rate in cell 27 first decreases with increasing concentrations of Gd > 1000 ppm and begins to increase at higher concentrations. The dose rate in cell 28 first decreases slightly, starting from a concentration of 100 ppm Gd, and then begins to increase. In cell 29, the dose rate increases with increasing Gd concentration and starting from 10,000 ppm, the dose rate decreases. Approximately such a picture of the change in the dose rate can be seen in cell 30. In the case of photons, one can see that the Gd concentration has a direct dependence on the dose, with an increase in the Gd concentration, the dose rate of photon radiation increases. The results obtained allow us to draw the following conclusions: When calculating the dose with Gd, it should be considered that in peripheral tumors the self-shielding effect begins to be influenced from 1000 ppm, in deeper tumors the self-shielding effect begins to influence even at low concentrations.

At high concentrations of Gd, the dose rate of photon radiation increases, which can be used for therapy. A more thorough study of this issue requires the continuation of these studies.

Acknowledgments

The authors are very grateful to Prof. Bazarov E. Kh for help and conditions created in the preparation of this study on the basis of the WWR-SM reactor of the Academy of Sciences of the Republic of Uzbekistan.

References:

1.G. Gambarini, D. Bettega, A. Gebbia, M. Felisi et al.,Uncertainties in the absorbed dose determination in irradiations with epithermalneutrons due to the dependence of neutron transport on shape and size ofthe exposed volume, ICNCT-18, Taipei, Taiwan, Abstrakt book , 2018, p.70-71.

2.Tooru Kobayashi, A practical handling of the limitation of absorbed dose in BNCT. ICNCT-18, Taipei, Taiwan, Abstract book , 2018, p.87-89.

3. A. Zaboronok, S. Taskaev, V. Kanygin, T. Bykovet al., Hybrid gold and boron nanoparticles for treatment and boron dose estimation inboron neutron capture therapy for malignant gliomaICNCT-18, Taipei, Taiwan, Abstract book , 2018, p.106-108.

4. H. Koivunoro, S. Gonzalez, L. Provenzano, L.Kankaanranta,H. Joensuu, Comparison of relative biological effectiveness (RBE) doses and the photon isoeffective dose model for predicting the normal tissue complication probability inboron neutron capture therapy (BNCT) of head and neck cancer patientsICNCT-18, Taipei, Taiwan, Abstract book , 2018, p.122-124.

5. S. Gonzalez, H. Koivunoro, L. Provenzano, C. Ferrariet al., How do photon iso-effective tumor doses derived from in-vitro BNCT studiescompare to those from in-vivo cancer model data?ICNCT-18, Taipei, Taiwan, Abstract book , 2018, p.126-128.
6. Sung-Joon Ye, Boron self-shielding effects on dose delivery of neutron capture therapy using epithermal beam and boronophenylalanine Medical Physics, Vol. 26, No. 11, November 1999, pp 2488-2493.
7. K. Pytel , K. Jozefowicz, B. Pytel and A. Kozieł Self-shielding effectsin neutron spectra measurements for neutron capture therapy by meanofactivation foils Radiation Protection Dosimetry (2004), Vol. 110, Nos 1-4, pp. 823---826doi:10.1093/rpd/nch134
8. S. A. Klykov Reaction Gd (n, γ) as a source of ionizing radiation for neutron capture therapy, PhD thesis, Obninsk, 2004
9. H. Koivunoro, L. Kankaanranta и H. T. Joensuu A Dose Response Analysis of Head and Neck Cancer Patients Treated with Boron Neutron Capture Therapy (BNCT) in Finland, The 17th International Congress on Neutron Capture Therapy, October 2-7, 2016, University of Missouri Columbia, Missouri, USA, Book of abstracts, 2016, p.45.
10. Asbury AK, Ojemann, Nielson SL, Sweet WH. Neuropathologic study of fourteen cases of malignant brain tumor treated by boron-10 slow neutron capture therapy. J Neuropathol Exp Neurol 1972;31:278-303.
11.Yamamoto T, Nakai K, Nariai T, Kumada H, Okumura T, Mizumoto M, Tsubo K, Zaboronok A, Ishikawa E, Aiyama H, et al: The status of Tsukuba BNCT trial: BPA-based boron neutron capture therapy combined with X-ray irradiation. Appl Radiat Isot 2011, 69:1817–1818.
12. Aiyama H, Nakai K, Yamamoto T, Nariai T, Kumada H, Ishikawa E, Isobe T, Endo K, Takada T, Yoshida F, et al: A clinical trial protocol for second line treatment of malignant brain tumors with BNCT at University of Tsukuba. Appl Radiat Isot 2011, 69:1819–1822.
13. Nakai K, Yamamoto T, Aiyama H, Takada T, Yoshida F, Kageji T, Kumada H, Isobe T, Endo K, Matsuda M, et al: Boron neutron capture therapy combined with fractionated photon irradiation for glioblastoma: a recursive partitioning analysis of BNCT patients. Appl Radiat Isot 2011, 69:1790–1792.
14.G. Abdullaeva, G. Djuraeva, A. Kim, Y. Koblik, G. Kulabdullaev, T. Rakhmonov, Sh. Saytjanov Evaluation of absorbed dose in Gadolinium neutron capture therapy Open Phys. 2015; 13:183 187.
15.ICRU 46, «Photon, Electron, Proton, and Neutron Interaction Data for Body Tissues, International Comission on Radiation Units and Measurements, Bethesda, MD, 1992.
16. G.A. Kulabdullaev et al., Uzb. Phys. J. 15, 127 (2013)
17. J. Stepanek, Radiation spectrum of 158Gd and radial dose distribution. In Advances in Neutron Capture Therapy 2 (B. Larsson, J. Crawford and R. Weinreich, Eds.). Excerpta Medica, Int. Cong. Series 1132, Elsevier, Amsterdam, 1997.
18.C. K. C Wang, M. Sutton, T. M. Evans and B. H. Laster, A microdosimetric study of $^{10}B(n,\alpha)^{7}Li$ and $^{157}Gd(n,\gamma)$ reactions for neutron capture therapy. In Proceedings of the Sixth International Radiopharmaceutical Dosimetry Symposium (A. T. Stelsen, M. G. Stabin and R. B. Sparks, Eds.), pp. 336–344. Report ORISE 99-0164, Oak Ridge Institute for Science and Education, Oak Ridge, TN, 1999.
19.T Goorley, H. Nikjoo, Electron and Photon Spectra for Three Gadolinium-Based Cancer Therapy Approaches. Radiat. Res. 54, 556–563 (2000).

20. M. Rivard, J. Stepanek Methods to determine the fluorescence and Auger spectra due to decay of radionuclides or due to a single atomic-subshell ionization and comparisons with experiments Med. Phys. 27, 1544 (2000).
21. S.A.Klykov, S.P.Kapchigashev, V.I.Potetnya et al. Experimental determination of energy release in the neutron capture by gadolinium. Atomnaya Energiya, v.91, i.6, December 2001.
22. Y.Sakurai, T.Kobayashi. Experimental Verification of the Nuclear Data of Gadolinium for Neutron Capture Therapy. Journal of NUCLEAR SCIENCE and TECHNOLOGY, Supplement 2, p. 1294-1297 (August 2002).
23. I. Sheino, V. Khokhlov, V. Kulakov, K. Zaitsev Estimation of neutron kerma in biological tissue containing boron and gadolinium compounds for neutron capture therapy Symposium,2004, Proseedings, pp.99-101.
24. MCNP - A General Monte Carlo NParticle Code - Version 4C. 2000. Briestmeister J.F.